CHIN. PHYS. LETT. Vol. 36, No. 12 (2019) 120701

Stress, Roughness and Reflectivity Properties of Sputter-Deposited B_4C Coatings for X-Ray Mirrors *

Jia-Li Wu(吴佳莉)[1,2], Run-Ze Qi(齐润泽)[2,3], Qiu-Shi Huang(黄秋实)[2,3], Yu-Fei Feng(冯宇飞)[2,3], Zhan-Shan Wang(王占山)[2,3]**, Zi-Hua Xin(辛子华)[1]**

[1]*Department of Physics, Shanghai University, Shanghai 200444*
[2]*MOE Key Laboratory of Advanced Micro-Structured Materials, Shanghai 200092*
[3]*Institute of Precision Optical Engineering, School of Physics Science and Engineering, Tongji University, Shanghai 200092*

(Received 27 May 2019)

Boron carbide (B_4C) coatings have high reflectivity and are widely used as mirrors for free-electron lasers in the x-ray range. However, B_4C coatings fabricated by direct-current magnetron sputtering show a strong compressive stress of about −3 GPa. By changing the argon gas pressure and nitrogen-argon gas mixing ratio, we are able to reduce the intrinsic stress to less than −1 GPa for a 50-nm-thick B_4C coating. It is found that the stress in a coating deposited at 10 mTorr is −0.69 GPa, the rms roughness of the coating surface is 0.53 nm, and the coating reflectivity is 88%, which is lower than those of coatings produced at lower working pressures. When the working gas contains 8% nitrogen and 92% argon, the B_4C coating shows not only −1.19 GPa stress but also a low rms roughness of 0.16 nm, and the measured reflectivity is 93% at the wavelength of 0.154 nm.

PACS: 07.85.Fv, 68.55.−a, 81.15.Cd DOI: 10.1088/0256-307X/36/12/120701

Single-layer mirrors are widely applied in free-election lasers (FELs) and synchrotron light sources.[1−2] For photon transmission systems, their reflective performance influences the beam alignment, focusing and imaging.[3−5] FELs possess ultra-high brightness and full coherence beams, and have produced important discoveries in the fields of physics, materials, and life sciences.[6−8] Due to the stringent specification of FELs, research of x-ray mirrors with excellent reflective performance is a considerable challenge. Boron carbide (B_4C) coatings are currently used as x-ray mirrors. B_4C is a promising coating material with high desirable properties such as superior stability, high hardness, and high damage threshold.[9−11] In addition, it has low absorption edge and can provide high reflectivity in the total reflection. These properties make it important for grazing-incidence mirrors in the photon energy range of operation.

B_4C is mostly utilized as a spacer or barrier layer in multilayers used in astronomy, EUV lithography, biological microscopy, and plasma diagnosis.[12−14] B_4C single layer or multilayer possess large compressive stress, which may cause delamination of the coatings.[10,14] Kulikovsky *et al.* deposited B_4C coatings 1.5-μm-thick on substrates that were either grounded or else biased at −100 V, and then they varied the annealing temperature.[15] The stress in the B_4C coatings decreased as the annealing temperature increased. Soufli *et al.* fabricated 50-nm-thick B_4C coatings under 10 mTorr Ar pressure for the linac coherent light source (LCLS) soft x-ray mirror offset system (SOMS) mirrors.[7] The intrinsic stress in the coating dropped from the original −2.5 GPa to −1.1 GPa as a result of optimizing the gas pressure. In the LCLS and the European XFEL, the optimum thickness of the B_4C coating was determined to be about 50 nm, to ensure good reflectivity and to suppress the higher harmonics of the FEL beam.[14,16−17]

Control of intrinsic stress can also be achieved by means of reactive sputtering with nitrogen, as previously demonstrated in W/B_4C, Pd/B_4C, Ru/B_4C and Co/C multilayers.[18−21] This method not only inhibits the interface diffusion but also improves thermal stability.[22] Some researchers believe that the incorporation of nitrogen has little effect on the optical constants of B_4C materials in the soft and hard x-ray bands.[18] In addition, high quality of surface morphology is required for good reflective performance.[23]

The first hard x-ray free-electron laser in China, called Shanghai High Repetition Rate Hard XFEL and Extreme Light Facility (SHINE), is under construction. The superconducting linac can produce electron beams with 8 GeV energy. After traversing through undulators, the emitted photons cover an energy range of 0.4–25 keV.[24,25] In this Letter, we focus on exploring the optimum deposition conditions, in particular, the sputtering Ar pressure and the N_2/Ar ratio, to fabricate B_4C single layers with low stress and low roughness for applications in FELs in the x-ray range. The evolution of stress and roughness of these B_4C coatings as the deposition conditions changes are discussed.

A series of test coupons were prepared, each consisting of a 50-nm-thick B_4C coating deposited on a D263 glass substrate (each 40 × 15 × 1 mm), a 5-nm-

*Supported by the National Key R&D Program of China under Grant No 2016YFA0401304, the National Natural Science Foundation of China under Grant Nos 61621001, U1732268 and 11875203, and the Shanghai Municipal Science and Technology Major Project under Grant No 2017SHZDZX02.
**Corresponding author. Email: wangzs@tongji.edu.cn; zhxin@staff.shu.edu.cn
© 2019 Chinese Physical Society and IOP Publishing Ltd

thick tungsten layer was deposited between the glass and the B_4C to improve the adhesion. All of the coatings were fabricated by the dc magnetron sputtering technique.[26] The deposition chamber was evacuated to a base pressure of less than 1×10^{-4} Pa, and each magnetron cathode was operated in the constant power mode at 100 W and 40 W for the B_4C and W targets, respectively. Two groups of B_4C coatings were deposited under different argon pressures with different nitrogen-argon gas mixtures. The first group consisted of B_4C coatings at variable Ar pressures of 1, 2.5, 5, and 10 mTorr, respectively. The second group included coatings deposited at various N_2/Ar ratios of 4%, 8% and 15%. For the second group, the working pressure was maintained constant at 1 mTorr during deposition.

Grazing incidence x-ray reflectivity (GIXRR) measurements were made in the 2θ–ω mode using an x-ray diffractometer (XRD) comprising a sealed-tube Cu anode and a Ge crystal monochromator tuned to the Cu K_α line (8.04 keV). Fitting of the measured XRR data was used to determine the coating thickness and roughness.

Roughness measurements were made using an atomic force microscope (AFM) and an optical profiler covering a wide range of spatial frequencies from 2×10^{-3} to $10^2\,\mu m^{-1}$. In the high spatial frequency range (HSFR), AFM scans of $1 \times 1\,\mu m^{-1}$ and $5 \times 5\,\mu m^{-1}$ were performed, and the data obtained were stored in a 256×256 pixel array. In the middle spatial frequency range (MSFR), optical profiler scans were performed with two objective lens magnifications, 10× and 50×, at each location, and the data from each scan were stored in a 640×480 pixel array.

The same series of B_4C coatings without the tungsten adhesive layer, deposited on polished quartz substrates in thickness of 1 mm thick and diameter of 3 mm, were used in the stress measurements. The film stress was measured with a Fizeau interferometer by detecting the changes in the curvature of the quartz substrates before and after the deposition. The stress value was calculated using the Stoney equation.[27] The film stress consists of thermal stress and intrinsic stress. We studied the latter stress, which is a large compressive stress. Although the thermal stress of B_4C coatings is a tensile stress, its value is negligible relative to the compressive stress and can be ignored.[28]

The surface quality of the coating is affected by the surface quality of the substrate. Therefore, it is necessary to ensure the lowest possible substrate roughness. The surface morphology of the uncoated substrate and the B_4C coating were characterized by optical profiler and by AFM. The power spectral density (PSD) was calculated to elucidate the roughness evolution versus spatial frequency.[10] The rms roughness σ_r can be obtained by

$$\sigma_r^2 = \int_{f_1}^{f_2} S(f_x) df_x, \tag{1}$$

where $S(f_x)$ is the surface one-dimensional PSD, f_1 and f_2 define the spatial frequency range of interest. For the HSFR, $f_1 = 1\,\mu m^{-1}$ and $f_2 = 1 \times 10^2\,\mu m^{-1}$, for the MSFR, $f_1 = 2 \times 10^{-3}\,\mu m^{-1}$ and $f_2 = 1\,\mu m^{-1}$.

The measured values were computed from the PSD curves according to Eq. (1) and were averaged between discrete locations on the surface. The PSD curve of the glass substrate is shown in Fig. 1 (solid line).

In addition, we computed $S(f_x)$ and fitted a power-law model in the form[29]

$$S(f_x) = \frac{K_n}{f_x^n}, \tag{2}$$

where K_n denotes spectral strengths and n denotes spectral indices.

The measured data and curve from the fitting model, with $K_n = 4.36 \times 10^{-9}\,\mu m^{3-n}$ and $n = 1.14$, are shown in Fig. 1 (dashed line), which demonstrates that the glass substrate possesses the well-known fractal behavior that can reduce its impact on film growth.[30]

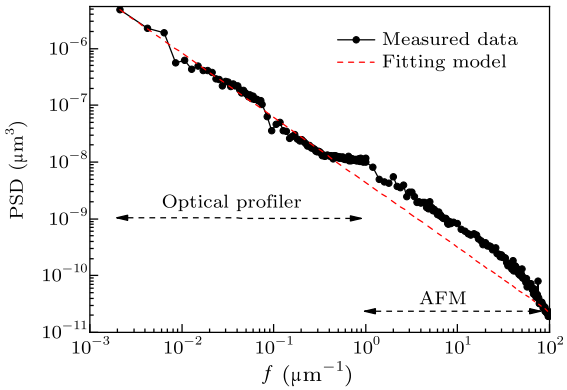

Fig. 1. PSD curve of a flat glass substrate. The solid line is the measured date, and the dashed line is from the fitting.

The measured roughness data covering the MSFR and HSFR are given in Table 1. From the test results of the optical profiler, it can be seen that the 1 mTorr B_4C coating improved the morphology of the glass substrate. Overall, the B_4C roughness increases with increasing working pressure, and it increases significantly in the AFM-measured range. In particular, in the scan of $1 \times 1\,\mu m^2$, the rms roughness of the B_4C coating increases from 0.16 nm to 0.53 nm when the Ar pressure changes from 1 mTorr to 10 mTorr.

The AFM $1 \times 1\,\mu m^2$ images (Figs. 2(a)–2(e)) show that the B_4C coatings deposited at 5 mTorr and 10 mTorr exhibit large voids and grains. With the increase of working pressure, the probabilities of collision/scattering between argon ions and the sputtering particles are increased.[31] Consequently, the energy of particles falling on the substrate is reduced. These porous columnar structures can relax the layer structure, which leads to an increase in roughness. It appears that the working pressure has a considerable influence on the layer structure.

Table 1. Values of rms roughness of the uncoated substrate and the B_4C coatings at different Ar pressures.

Sample	Magnification 10× (nm)	Magnification 50× (nm)	Scan $5\times5\,\mu m^2$ (nm)	Scan $1\times1\,\mu m^2$ (nm)
Glass substrate	0.32	0.30	0.17	0.16
1 mTorr Ar	0.23	0.21	0.18	0.17
2.5 mTorr Ar	0.26	0.28	0.19	0.18
5 mTorr Ar	0.36	0.28	0.23	0.26
10 mTorr Ar	0.35	0.29	0.45	0.53

To understand the surface morphology of the B_4C coatings, PSD curves are shown in Fig. 3. It can be seen that varying the Ar pressure during deposition of the B_4C coatings mainly affects the HSFR for spatial frequencies greater than $1\,\mu m^{-1}$. In the MSFR, the B_4C coatings nearly replicate the topography of the glass substrate.

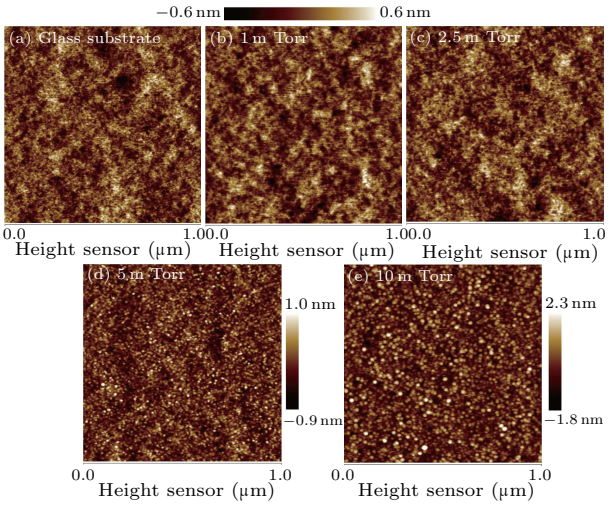

Fig. 2. (a)–(e) Results for substrate and the coating morphologies. HSFR values were measured with an AFM in a scan of $1\times1\,\mu m^2$.

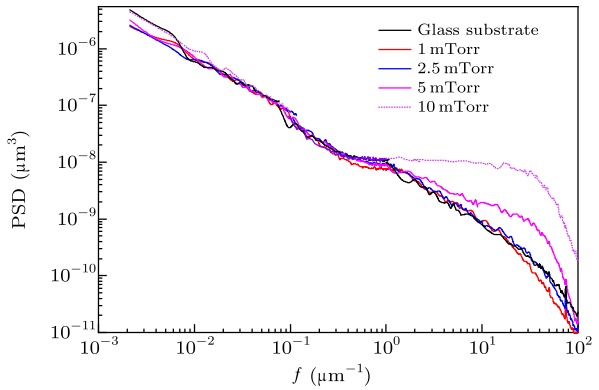

Fig. 3. One-dimensional PSD function of B_4C coatings at different Ar pressures.

Figure 4 shows the stress of the B_4C coatings fabricated at different Ar pressures. It is demonstrated that with the increasing working pressure, the changes in stress and roughness trend in opposite directions as functions of argon pressures. Coatings deposited at sufficiently low pressures were in a state of high compression. As the working pressure increases from 1 to 10 mTorr, the compressive stress of the B_4C coating gradually decreases from −3.06 GPa to −0.69 GPa. This is similar to the previously reported results of Soufli *et al.*[7] This inverse correlation between film stress and surface roughness can be described by structure-zone models with the low temperature ($T/T_m < 0.3$).[32] The low-pressure sputtered films are characterized by a zone T-type microstructure comprising over-dense columnar structure with large compressive stresses, as the pressure increases, the films possess loose columnar structure with lower stresses, or even tensile stresses. We term this a zone-1-type microstructure comprising of porous material with large surface roughness.

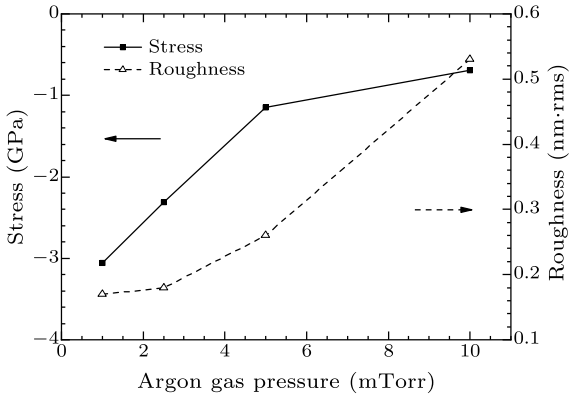

Fig. 4. Stress of the B_4C coatings fabricated at different Ar pressures (solid squares). The rms roughness of the same samples were measured with an AFM in a scan of $1\times1\,\mu m^2$ (hollow triangles).

The change of stress can also be explained by the atomic peening effect of energetic particles on the growing film. Lower gas pressures result in bombardment of the film surface by highly energetic particles, resulting in the growth of compact films with compressive stress. Meanwhile, higher gas pressures cause less atomic peening, which results in less compact films containing a larger number and size of atomic-scale voids. These voids allow the compressive stress to relax towards the tensile direction.[32] Under pure argon conditions, boron mainly exists in the elemental form, but a small amount exists in the form of the compounds B_4C and B_2O_3.[20] Interstitial atoms like Ar could exist in the voids between the columns.

As the working pressure was increased to 10 mTorr, the pure B_4C deposition rate decreased from 2.91 nm/min to 2.14 nm/min due to the reduced mean free path and the enhanced scattering collisions of the depositing atoms. The x-ray reflectivity (at the Cu K_α line) of a B_4C coating deposited at 1 mTorr is about 95% at incidence angles of about 0.22 deg, and the film density is about $2.39\,g/cm^3$. For the B_4C coatings deposited at 2.5 mTorr or 5 mTorr, the reflectivity

is about 92%. However, for the 10 mTorr B_4C coating, the reflectivity deceases to 88%.

As shown in Table 2, the roughness of the B_4C coatings increased slightly as the working nitrogen gas ratio increased from 4% to 15% in the HSFR and MSFR. At an N_2 ratio of 4%, the B_4C coating shows the smallest roughness. Compared with the uncoated substrate, there is no obvious change in the surface morphology of B_4C coatings that were fabricated at different N_2 ratios, even under a 15% N_2 ratio. These results are consistent with those shown in the corresponding PSD curves in Fig. 5.

Table 2. Values of rms roughness of B_4C coatings at different nitrogen/argon gas mixture ratios.

Sample	Magnification 10× (nm)	Magnification 50× (nm)	Scan $5 \times 5\,\mu m^2$ (nm)	Scan $1 \times 1\,\mu m^2$ (nm)
96%Ar+4%N_2	0.28	0.22	0.18	0.15
92%Ar+8%N_2	0.32	0.22	0.18	0.16
85%Ar+15%N_2	0.33	0.23	0.18	0.17

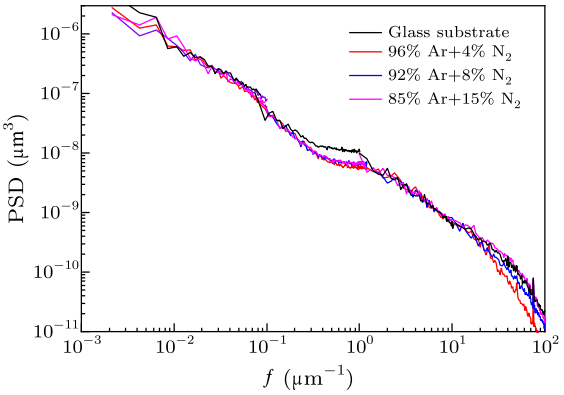

Fig. 5. One-dimensional PSD function of B_4C coatings obtained at different nitrogen/argon gas ratios.

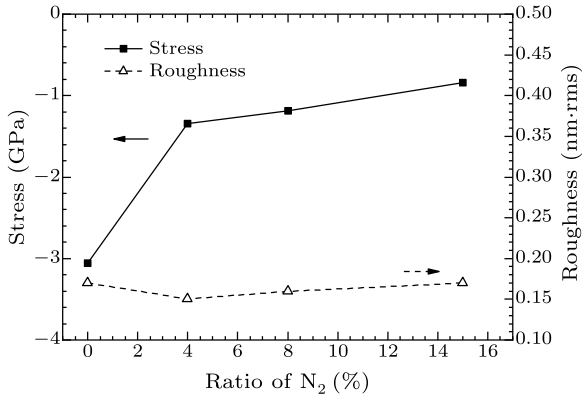

Fig. 6. Stress of the B_4C coatings fabricated at different nitrogen/argon gas ratios (solid squares). The rms roughness of the same samples were measured with an AFM in a scan of $1 \times 1\,\mu m^2$ (hollow triangles).

The stress measurement results for the nitrided samples are shown in Fig. 6. There was a sharp and significant reduction in stress in the nitrided B_4C coatings compared to the pure B_4C coatings, which demonstrates that nitrogen addition can dramatically reduce the stress of the coatings. The B_4C coating fabricated with pure Ar exhibits a large compressive stress of −3.09 GPa. After adding 4% or 8% N_2 to the working gas, the stress was significantly reduced to −1.34 GPa or −1.19 GPa, respectively. With a higher N_2 ratio of 15%, the stress further decreased down to −0.84 GPa. For these nitrided B_4C single layers, the trend of the stress reduction is similar to the earlier reported results of Windt *et al.*[18]

To clarify the influence of nitrogen on the film stress, we analyzed the elemental valence and atomic fraction of coatings with x-ray photoelectron spectroscopy (XPS). In Fig. 7(a), the B 1*s* central peak locates at about 188.6 eV, corresponding to B–C bonds.[13,33] The peaks at the binding energy of 189.4 eV and 191 eV corresponding to elemental state of boron and oxides, respectively.[20,34,35]

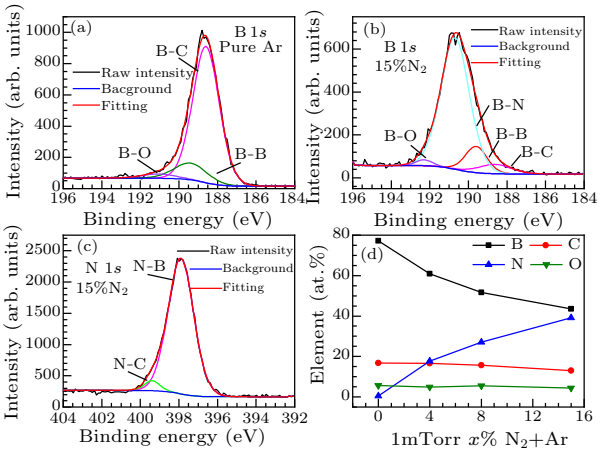

Fig. 7. (a) B 1*s* spectrum of the B_4C coating deposited with pure Ar. (b) B 1*s* and (c) N 1*s* spectra of the nitrided coating deposited with N_2 ratio of 15%. (d) Atomic fraction of B, C and N for the B_4C coatings deposited with N_2 ratio of 15%.

Figures 7(b) and 7(c) show the B 1*s* and N 1*s* spectra for the B_4C coatings with N_2 ratio of 15%. Compared with the B 1*s* spectrum of the B_4C coating deposited with pure Ar, the B 1*s* peak of the nitrided B_4C coating shifts to higher binding energy. In Ref. [32], the peak centered at 190.7 eV was fitted with B–N bonds. Small peaks at 189.6 eV and 188.6 eV were attributed to elemental boron and B_4C, respectively. The ones at higher binding energy are identified at more than 192 eV, corresponding to BC_2O, BCO_2 and B_2O_3.[36] The atomic fraction of boron in the chemical states of nitrides is 79%, while in the chemical states of carbides it is dramatically decreased down to 7%. The N 1*s* central peak located at about 397.9 eV corresponds to N–B bonds.[20,33] A small peak at energy of 399.4 eV was fitted to N–C bonds.[20,36] Figure 7(d) shows the atomic concentration of the boron, carbon and nitrogen in the nitrided B_4C coatings. The ratio of B/C is close to 4:1 for B_4C coating under pure Ar pressure. However, as the proportion of nitrogen in-

creased, this ratio decreased dramatically to ∼3.3 at N_2 ratio of 15%. Meanwhile, the increasing concentration of nitrogen atoms was apparently observed.

In the composition analysis of nitrided B_4C coatings, we found that the B–C bonds decreased significantly, accompanied by formation of B–N bonds. The bonding mode of boron atoms was mainly B–N bonds, but no longer B–C bonds. Thus, it can be concluded that most nitrogen atoms react with boron atoms to form boron nitride (BN) compounds, decreasing the content of B_4C. This change trend of B_4C content is similar to that of stress. In the nitrided B_4C coating, the chemical environment and the bonding structure of boron atoms have changed. Different from the change of working pressure, nitrogen filling not only reduces the stress but also smooths the surface of the film.

In addition, a large increase in B_4C deposition rate with the nitrogen ratio was observed, and the deposition rate of B_4C coating at an N_2 ratio of 15% was 4.20 nm/min, which is advantage for the given low deposition rate of pure B_4C. For the B_4C coatings deposited at 4% N_2 or 8% N_2, the reflectivity is about 93%. Upon adding more nitrogen to the sputtering gas, the reflectivity decreases to 87%. Owing to the essentially relaxed stress and lower roughness, preparation of the B_4C coating with a ratio of 8% N_2 can be of interest for practical applications.

In conclusion, to preserve high reflectivity and a perfect x-ray wavefront, we have investigated different deposition conditions including the working pressure and the composition of the working gas to achieve both low stress and low roughness of B_4C coatings. A gas mixture with 8% N_2 and 92% Ar is found to be the appropriate condition for generating B_4C coatings with $\leq$0.32 nm roughness and −1.19 GPa stress. This will be of practical interest if further studies can show good thermal stability. Nevertheless, when working under the ultra-intense FEL beam, the stress value is too high to withstand the long-time multi-pulse exposure. Thus, using an optimized working pressure or gas mixture is not sufficient to reduce the intrinsic stress of B_4C films. Further consideration of other techniques, such as annealing, will be required to obtain a B_4C coated mirror with high reflectivity and lower stress than those achieved presently.

References

[1] Störmer M, Horstmann C, Siewert F et al 2010 *AIP Conf. Proc.* (Melbourne Australia 27 September–2 October 2009) **1234** 756

[2] Jacobi S, Steeg B, Wiesmann J et al 2002 *Proc. SPIE* (Seattle WA USA 7–11 July 2002) **4782** 113

[3] Barty A, Soufli R, McCarville T et al 2009 *Opt. Express* **17** 15508

[4] Flechsig U, Bahrdt J, Follath R and Reiche S 2016 *AIP Conf. Proc.* (New York, USA 6–10 July 2015) **1741** 040040

[5] Störmer M, Siewert F and Gaudin J 2011 *Proc. SPIE* (Prague Czech Republic 18–21 April 2011) **8078** 80780G

[6] Soufli R, Fernández-Perea M, Hau-Riege S P et al 2011 *Proc. SPIE* (Prague Czech Republic 18–21 April 2011) **8077** 807702

[7] Soufli R, Pivovaroff M J, Baker S L et al 2008 *Proc. SPIE* (San Diego California USA 10–14 August 2008) **7077** 707716

[8] Milne C J, Schietinger T, Aiba M et al 2017 *Appl. Sci.* **7** 720

[9] Hau-Riege S P, London R A, Bionta R M et al 2009 *Appl. Phys. Lett.* **95** 111104

[10] Pivovaroff M J, Bionta R M, Mccarville T J, Soufli R and Stefan P M 2007 *Proc. SPIE* (San Diego California USA 26–30 August 2007) **6705** 67050O

[11] Barthelmess M and Bajt S 2011 *Proc. SPIE* (Prague Czech Republic 18–21 April 2011) **8077** 807710

[12] Morawe Ch, Supruangnet R and Ch J 2015 *Thin Solid Films* **588** 1

[13] Jiang H, Zhu J, Huang Q et al 2011 *Appl. Surf. Sci.* **257** 9946

[14] Soufli R, Baker S L, Robinson J C et al 2009 *Proc. SPIE* (Prague Czech Republic 20–23 April 2009) **7361** 73610U

[15] Kulikovsky V, Vorlicek V, Ctvrtlik R, Bohac P and Lapsanska H 2011 *Surf. Coat. Technol.* **205** 4052

[16] Störmer M, Siewert F, Horstmann C, Buchheim J and Gwalt G 2018 *J. Synchrotron Rad.* **25** 116

[17] Störmer M, Siewert F and Sinn H 2016 *J. Synchrotron Rad.* **23** 50

[18] Windt D L 2007 *Proc. SPIE* (San Diego California USA 26–30 August 2007) **6688** 66880R

[19] Wang Y, Huang Q, Yi Q et al 2017 *Opt. Express* **25** 7749

[20] Huang Q, Liu Y, Yang Y et al 2018 *Opt. Express* **26** 21803

[21] Bellotti J A and Windt D L 2009 *Proc. SPIE* (San Diego California USA 2–6 August 2009) **7437** 743715

[22] Hultman L 2000 *Vacuum* **57** 1

[23] Soufli R, Fernández-Perea M, Baker S L et al 2012 *Appl. Opt.* **51** 2118

[24] Li K and Deng H 2018 *Nucl. Inst. Methods Phys. Res. Sect. A* **895** 40

[25] Lv H, Leng Y, Yan Y and Wang H 2018 *Nucl. Inst. Methods Phys. Res. Sect. A* **908** 167

[26] Panahi N et al 2016 *Chin. Phys. Lett.* **33** 066802

[27] Stoney G G 1909 *Proc. R. Soc. London Ser. A* **82** 172

[28] Morawe C, Ch J and Friedrich K 2010 *Proc. SPIE* (San Diego California USA 1–5 August 2010) **7802** 78020B

[29] Church E L, Takacs P Z and Leonard T A 1989 *Proc. SPIE* (San Diego, USA 7–11 August 1989) **1165** 136

[30] Church E L 1988 *Appl. Opt.* **27** 1518

[31] Niibe M, Nii H and Sugie Y 2002 *Jpn. J. Appl. Phys.* **41** 3069

[32] Thornton J A 1986 *J. Vac. Sci. & Technol. A* **4** 3059

[33] Moulder J F, Stickle W F, Sobol P E and Bomben K D 1995 *Handbook of X-Ray Photoelectron Spectroscopy* (USA: Physical Electronics Inc) pp 215–230

[34] Li P, Huang Q, Jiang L et al 2016 *Vacuum* **128** 85

[35] Soufli R, Aquila A L, Salmassi F, Fernández-Perea M and Gullikson E M 2008 *Appl. Opt.* **47** 4633

[36] Prakash A and Sundaram K B 2017 *Appl. Surf. Sci.* **396** 484